


# DHA induces ER stress and growth arrest in human colon cancer cells: associations with cholesterol and calcium homeostasis<sup>§</sup>

Caroline Hild Jakobsen,<sup>1,\*</sup> Gro Leite Størvold,<sup>1,\*,††</sup> Hilde Bremseth,<sup>1,†</sup> Turid Follestad,<sup>§</sup> Kristin Sand,<sup>\*\*</sup> Merete Mack,<sup>\*</sup> Karina Standahl Olsen,<sup>†</sup> Anne Gøril Lundemo,<sup>\*</sup> Jens Gustav Iversen,<sup>2,\*\*</sup> Hans Einar Krokan,<sup>†</sup> and Svanhild Arentz Schönberg<sup>3,\*</sup>

Departments of Laboratory Medicine, Children's and Women's Health,<sup>\*</sup> Cancer Research and Molecular Medicine,<sup>†</sup> Mathematical Sciences,<sup>§</sup> Norwegian University of Science and Technology (NTNU), Erling Skjalgssons gate 1, N-7006 Trondheim, Norway; Institute of Basic Medical Sciences,<sup>\*\*</sup> Department of Physiology, Domus Medica, University of Oslo, Gaustad, Sognsvannsveien 9, 0372 Oslo, Norway; and Department of Medical Genetics,<sup>††</sup> Ullevål University Hospital, Faculty of Medicine, University of Oslo, 0318 Oslo, Norway

**Abstract** Polyunsaturated fatty acids (PUFAs) are normal constituents of the diet, but have properties different from other fatty acids (e.g., through generation of signaling molecules). N-3 PUFAs reduce cancer cell growth, but no unified mechanism has been identified. We show that docosahexaenoic acid (DHA; 22:6 n-3) causes extensive changes in gene expression patterns at mRNA level in the colon cancer cell line SW620. Early changes include unfolded protein response (UPR) and increased levels of phosphorylated eIF2 $\alpha$  as verified at protein level. The latter is considered a hallmark of endoplasmic reticulum (ER) stress and is abundantly present already after 3 h. It may coordinate many of the downstream changes observed, including signaling pathways for cell cycle arrest/apoptosis, calcium homeostasis, cholesterol metabolism, ubiquitination, and proteasomal degradation. Also, eicosapentaenoic acid (EPA), but not oleic acid (OA), induced key mediators of ER stress and UPR at protein level. Accumulation of esterified cholesterol was not compensated for by increased total levels of cholesterol, and mRNAs for cholesterol biosynthesis as well as de novo synthesis of cholesterol were reduced.  These results suggest that cytotoxic effects of DHA are associated with signaling pathways involving lipid metabolism and ER stress.—Jakobsen, C. H., G. L. Størvold, H. Bremseth, T. Follestad, K. Sand, M. Mack, K. S. Olsen, A. G. Lundemo, J. G. Iversen,

H. E. Krokan, and S. A. Schönberg. **DHA induces ER stress and growth arrest in human colon cancer cells: associations with cholesterol and calcium homeostasis.** *J. Lipid Res.* 2008. 49: 2089–2100.

**Supplementary key words** gene expression • phosphorylated eIF2 $\alpha$  • antioxidant response • heat shock response • cytosolic free Ca<sup>2+</sup> • cell cycle • total cholesterol level • cholesterol synthesis

Long-chain polyunsaturated fatty acids (PUFAs) of the n-3 type are important dietary components that may prevent or alleviate coronary heart disease and inflammatory conditions (1, 2). Even though epidemiological studies on the association between fish consumption and cancer risk are not consistent, evidence from animal- and cell-culture studies demonstrate that PUFAs inhibit cancer-cell growth, induce apoptosis, and increase the efficiency of chemotherapeutic drugs (3–5). Several mechanisms have been proposed for the antiproliferative effect of n-3 PUFAs; among these are alterations in eicosanoid formation (6), lipid peroxidation initiated by free radicals (7–9), accumulation of cytotoxic lipid droplets (10), and specific changes in gene expression patterns (11, 12). This could be mediated directly by PUFAs as ligands of transcription factors, or indirectly through metabolites of PUFAs or other secondary events. There is evidence indicating that fatty acids may regulate gene expression directly. The activity and

The project was financed by The Faculty of Medicine, NTNU, The Cancer Research Fund, Trondheim University Hospital, and The Research Council of Norway through grants from the Functional Genomics Program (FUGE). Microarray experiments were performed at the microarray core facility at the Norwegian Microarray Consortium (NMC), Trondheim, which is supported by FUGE, The Norwegian Research Council. Financial support was also given by the cross-disciplinary project "BIOEMIT-Prediction and modification in functional genomics: combining bioinformatical, bioethical, biomedical, and biotechnological research," NTNU.

\* Author's Choice—Final version full access.

Manuscript received 19 August 2007 and in revised form 15 January 2008 and in re-revised form 3 June 2008 and in re-re-revised form 19 June 2008.

Published, JLR Papers in Press, June 19, 2008.  
DOI 10.1194/jlr.M700389.JLR200

Copyright © 2008 by the American Society for Biochemistry and Molecular Biology, Inc.

This article is available online at <http://www.jlr.org>

<sup>1</sup>C. H. Jakobsen, G. L. Størvold, and H. Bremseth contributed equally to this work.

<sup>2</sup>Deceased.

<sup>3</sup>To whom correspondence should be addressed.

e-mail: [svanhild.schonberg@ntnu.no](mailto:svanhild.schonberg@ntnu.no)

<sup>§</sup>The online version of this article (available at <http://www.jlr.org>) contains supplementary data.

abundance of several nuclear transcription factors, like peroxisome proliferator-activated receptors (PPAR $\alpha$ / $\delta$ / $\gamma$ ), liver X receptors (LXR $\alpha$ / $\beta$ ), and sterol regulatory element-binding proteins (SREBP1/2), have been shown to be regulated by dietary PUFAs and their metabolites (11, 13).

Cellular stress from cytotoxic agents may result in adaptive mechanisms in several cellular compartments, including endoplasmic reticulum (ER). ER has three main functions: 1) folding, glycosylation, and sorting of proteins to their proper destination; 2) synthesizing cholesterol and other lipids; and 3) maintenance of Ca<sup>2+</sup> homeostasis. Disruption of any of these processes causes ER stress and activates the unfolded protein response (UPR). The UPR up-regulates genes that support adaptation to and recovery from ER stress as well as initiating apoptotic pathways when damage is severe. Three transmembrane proteins mediate the UPR signal across the ER membrane: inositol-requiring enzyme 1 (IRE1), eukaryotic translation initiation factor 2 $\alpha$  (eIF2 $\alpha$ ) kinase 3 (EIF2AK3/PKR-like ER kinase [PERK]), and activating transcription factor 6 (ATF6). PERK belongs to a family of eIF2 $\alpha$  kinases that regulates the translational control during the UPR. Phosphorylation of eIF2 $\alpha$  by PERK leads to attenuation of global protein synthesis, but promotes translation of certain mRNAs, like activating transcription factor 4 (ATF4) mRNA (14). Downstream targets of ATF4 are *CHOP*, *GADD34*, *ATF3*, and genes involved in amino acid metabolism, glutathione biosynthesis, resistance to oxidative stress, and protein secretion. Loss of cyclin D1 during ER stress leads to G1 arrest and provides the cell with an opportunity to restore cell homeostasis (15). However, prolonged ER stress may cause cell death. ER stress-induced apoptosis may be mediated by caspase-12, caspase-9, and caspase-7 (16).

Several links exist between signaling pathways controlling the UPR and lipogenesis. Activation of the transcription factors ATF6 as well as the SREBPs that control cholesterol and lipid synthesis requires translocation from the ER to the Golgi followed by cleavage by site-1 protease (S1P) and site-2 protease (S2P) (17). Also, ER stress may activate expression of genes involved in cholesterol biosynthesis (18, 19). Both elevated levels of cholesterol as well as depletion have been shown to induce ER stress (20, 21).

We have previously shown that the human colon cancer cell lines SW480 and SW620, derived from a primary and a secondary tumor of the same patient, respectively, were strongly growth inhibited by docosahexaenoic acid (DHA) (5). DHA enhanced lipid peroxidation in both cell lines significantly, measured as accumulation of the end product malondialdehyde. The antioxidant vitamin E ( $\alpha$ -tocopherol) completely abolished the increase in malondialdehyde, without restoring cell growth, demonstrating that the cells were resistant to lipid peroxidation products. DHA accumulated mainly as triglyceride and cholesteryl ester-enriched lipid droplets in SW480 and SW620, respectively. The protein level of the nuclear form of SREBP1 (nSREBP1) decreased in both cell lines, indicating a possible relationship between disturbances in lipid homeostasis and cell-cycle arrest. We demonstrate that DHA-treatment of SW620 cells results in extensive changes in gene expres-

sion patterns at the mRNA level. Early changes include induction of ER stress, as evident from the abundant presence of phosphorylated eIF2 $\alpha$  (eIF2 $\alpha$ -P); increase in cytosolic Ca<sup>2+</sup>; and disturbances in lipid metabolism. Downstream signaling subsequently results in growth arrest and protein degradation. Key mediators of ER stress, eIF2 $\alpha$ -P, as well as ATF4 were also induced by eicosapentaenoic acid (EPA), but not by oleic acid (OA) treatment.

## MATERIALS AND METHODS

### Cell culture and fatty acid treatment

Human colon adenocarcinoma cell line, SW620, was obtained from American Type Culture Collection (Rockville, MD). Cells were cultured in Leibovitz's L-15 medium (Cambrex, BioWhittaker, Walkersville, MD) supplemented with L-glutamine (2 mM), FBS (10%), and gentamicin (45 mg/l) (complete growth medium) and maintained in a humidified atmosphere of 5% CO<sub>2</sub>: 95% air at 37°C. Stock solutions of DHA, EPA, and OA in ethanol (Cayman Chemical, Ann Arbor, MI) were stored at -20°C and diluted in complete growth medium before experiments (final concentration of ethanol < 0.025% v/v).

### RNA isolation

Seeded in 75 cm<sup>2</sup> flasks were 1.5 × 10<sup>6</sup> cells. After 8 h, complete growth medium supplemented with DHA (70  $\mu$ M) or an equal volume of ethanol (control) was added, and cells were incubated for 12, 24, and 48 h. Cells were harvested by scraping in ice-cold phosphated buffered saline (PBS) and stored at -80°C. Total RNA was isolated using the High Pure RNA Isolation Kit (Roche, Mannheim, Germany) according to instruction manual. RNase inhibitor rRNasin (40U/ $\mu$ l, 1  $\mu$ l) (Promega, Madison, WI) was added, and RNA was up-concentrated on a speed vac and resuspended in RNase free distilled H<sub>2</sub>O. RNA concentration and quality were determined using the NanoDrop1000 (NanoDrop Technologies, Wilmington, DE) and agarose gel electrophoresis.

### Gene expression profiling

Five micrograms total RNA was used for cDNA and cRNA synthesis according to the eukaryote expression manual (Affymetrix, Santa Clara, CA). Detailed gene expression profiling procedure can be found in supplementary data. cRNA was hybridized to the Human Genome Focus Array (Affymetrix). Washing and staining were performed using the Fluidics Station 400 (Midi-Euk2v3 protocol). The arrays were scanned using an Affymetrix GeneChip GA2500 Scanner, controlled by GeneChip<sup>®</sup> Operating Software 1.2 (GCOS, Affymetrix). Expression profiling was performed in triplicates at all time points using RNA from independent biological replicates. All experiments have been submitted to Array-Express with accession number E-MEXP-1014.

### Statistical analysis of gene expression data

Statistical analysis was performed based on summary expression measures for each probe set of the GeneChips, using the raw data (CEL) files and a linear statistical model for background-corrected, quantile normalized, and log-transformed perfect match values, performed by the robust multiarray average (RMA) method (22, 23).

For each transcript, a linear regression model including parameters representing treatment effects and time effects for the treatment group was fitted to the RMA expression measures. Based on the estimated effects, tests for significant differential ex-

pression due to DHA treatment were performed using moderated t-tests, in which gene-specific variance estimates are replaced by variance estimates found by borrowing strength from data on the remaining genes (24).

To account for multiple testing, adjusted *P* values controlling the false discovery rate were calculated (25) by inserting the estimated value of the proportion of nondifferentially expressed genes (26). Differentially expressed genes were selected based on a threshold of 0.05 on the adjusted *P* values.

Time effect in the control groups were considered negligible and omitted from the model. Statistical analysis was performed in R (27), using the packages Limma and affy from Bioconductor (28). Differentially expressed genes were annotated using the NetAffx Analysis Centre (<http://www.Affymetrix.com>) and NMC Annotation Tool/eGON V2.0 (<http://www.GeneTools.no>).

### Immunoblot analysis

DHA treatment of cells and preparation of total protein extracts were performed as described previously (5). Nuclear extracts for detection of ATF4 were prepared using a Nuclear extract kit (Active Motif, Belgium) according to manufacturer's instructions. To detect phosphorylated eIF2 $\alpha$ , cells were washed and scraped in ice-cold PBS-1 mM EDTA and pelleted by centrifugation. Pellets were lysed in 2  $\times$  packed cell volumes of lysis buffer on ice for 10 min. Equal amounts of protein were separated on 10% precast denaturing NuPAGE gels (Invitrogen, Carlsbad, CA) and transferred to polyvinylidene difluoride membranes (Millipore, Billerica, MA). The blots were incubated with the indicated primary and horse radish peroxidase-conjugated secondary antibodies (DAKO, Carpinteria, CA) and detected by chemiluminescence using Super Signal West Femto Maximum Sensitivity Substrate (Pierce, Rockford, IL) and visualized by Kodak Image Station 4000R (Eastman Kodak Co., Rochester, NY). Quantification was performed using Kodak Molecular Imaging Software (version 4.0.1). Details about buffers and primary antibodies can be found in the supplementary data.

### Measurement of cytosolic calcium in single cells

Cytosolic free Ca<sup>2+</sup> in single cells was determined as previously described (29). In short, cells were incubated for 40 min at 37°C with a solution of 5  $\mu$ M fura-2, 0.25% DMSO, and 0.025% Pluronic F-127 (TefLab, Austin, TX) in HEPES-buffered salt solution (HSS). Cells were then washed once and incubated in 400  $\mu$ l HSS. Applications to cells were done by injecting 100  $\mu$ l of agonist into the well. Ca<sup>2+</sup> imaging and registration software has been developed by Rotnes and Iversen (30). Cytosolic Ca<sup>2+</sup> concentration was calculated using the equation:  $[Ca^{2+}] = K_d\beta(R - R_{min}) / (R_{max} - R)$  (31). Fluorescence data were analyzed using the program LICCS (32).

### Analysis of total cholesterol levels

Seeded in 175 cm<sup>2</sup> flasks were 4  $\times$  10<sup>6</sup> cells. The following day, medium was replaced with complete growth medium supplemented with DHA (70  $\mu$ M) or medium with equal volume of ethanol and harvested after 3, 6, 12, 24, and 48 h incubation. Cells were harvested by trypsination and resuspended in PBS together with floating cells collected by centrifugation. The cell suspension was counted using a Coulter Counter (Beckman Coulter, Fullerton, CA) and an aliquot of 4  $\times$  10<sup>6</sup> cells was collected by centrifugation. Lipids were extracted from the cell pellet (33) using chloroform-methanol-water (1:2:0.8 v/v/v). Total cholesterol levels (cholesteryl ester and free cholesterol) in the lipid extracts were determined using the Amplex Red Cholesterol Assay Kit (Invitrogen) according to the instruction manual. Data were expressed as  $\mu$ g cholesterol/mg protein.

### Analysis of cholesterol and cholesteryl ester synthesis

Seeded in 175 cm<sup>2</sup> flasks were 4  $\times$  10<sup>6</sup> cells. The following day, medium was replaced with complete growth medium supplemented with DHA (70  $\mu$ M) or with equal volume of ethanol (control) and incubated for 24 h. Cells were then incubated with complete growth medium containing <sup>14</sup>C-acetate (1.2  $\mu$ Ci/ml) and DHA (70  $\mu$ M) or ethanol (control cells) for 4 and 6 h. Cells (12  $\times$  10<sup>6</sup>) were harvested by trypsination, and cellular lipids were extracted with chloroform/methanol according to a method modified after Bligh and Dyer (33). Lipids were separated by thin layer chromatography using hexane/diethyl ether/acetic acid (70:30:1, v/v/v) and lipids were visualized using iodine vapor. Lipid fractions were solubilized in Insta-gel plus (Perkin Elmer) before counting. Data were expressed as incorporation of <sup>14</sup>C-acetate into cholesterol/cholesteryl ester (cpm/mg protein).

## RESULTS

### Growth inhibition by DHA through ER stress and growth arrest signaling

The human colon cancer cell line SW620 is strongly growth-inhibited by DHA. Between 72 h and 144 h, essentially no growth could be observed after treatment with 70  $\mu$ M DHA (5). Although growth retardation was modest after 24 h, [<sup>3</sup>H]thymidine incorporation was reduced 30–40% in SW620 cells already by 12 h, while no effect was observed after 6 h (data not shown).

We demonstrate that complex gene networks and cell signaling pathways are affected at the mRNA level after DHA treatment in SW620 cells (**Fig. 1 and Table 1**). The number of transcripts differentially expressed increased from 12 to 24 h of DHA treatment [up-regulated: 839 (12 h) vs. 1157 (24 h); down-regulated: 1066 (12 h) vs. 1222 (24 h)], while the number decreased at 48 h (up-regulated: 288; down-regulated: 267). The fold change of transcript levels after DHA treatment ranged from 1.2 to 24, the majority of which being toward the lower end. Transcripts could be classified into several functional categories after annotation as shown in Table 1 and outlined in later discussion. More comprehensive information on changes in gene expression is found in the supplementary Table I. Early changes include induction of ER stress and UPR.

The protein levels of selected target genes were measured in SW620 cells after DHA treatment. Importantly, we demonstrate that an abundant amount of eIF2 $\alpha$ -P is found as early as 3 h after DHA treatment, preceding the activation of ATF4 and HMOX1 (**Fig. 2A**). Phosphorylation of eIF2 $\alpha$  is considered a hallmark of the UPR and ER stress and leads to attenuation of global protein synthesis, but promotes translation of certain mRNAs, like ATF4 mRNA (15). In accordance with this, ATF4 is up-regulated here both at the mRNA and protein level (Table 1 and Fig. 2A). Downstream targets of ATF4, *ATF3*, and genes involved in amino acid metabolism (*ASNS*), glutathione biosynthesis, resistance to oxidative stress (*HMOX1*), and protein secretion are up-regulated at the mRNA level and (when examined) at the protein level (Fig. 2A, Table 1 and supplementary Table I). Also, ATF6, PERK, and X-box binding protein 1



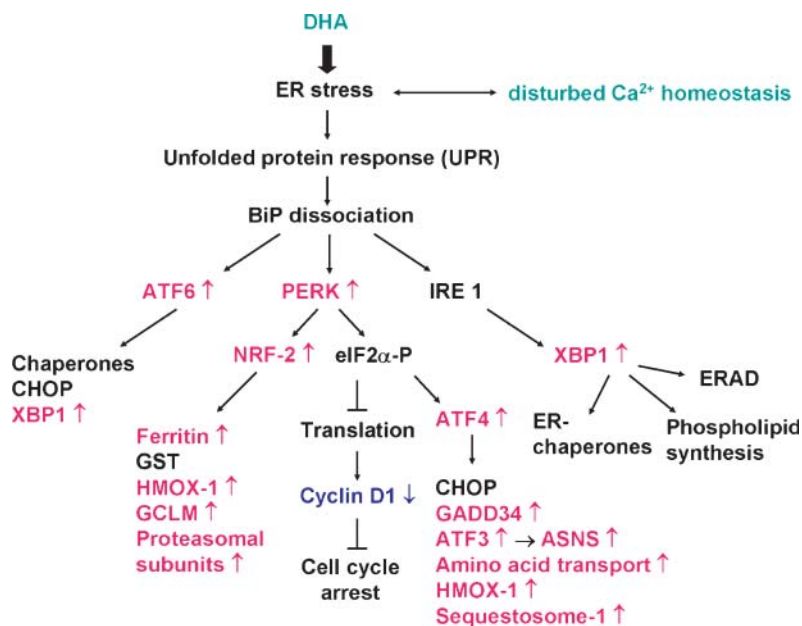


**Fig. 1.** Docosahexaenoic acid (DHA) induces endoplasmic reticulum (ER) stress in SW620 cells. Diagram showing transcripts found to be affected by DHA treatment in SW620 cells by gene expression analysis (up-regulated, pink; down-regulated, blue) in the main pathways of ER stress signaling. Three transmembrane proteins mediate the unfolded protein response (UPR) across the ER membrane after dissociation from BiP, activating transcription factor 6 (ATF6), PERK, and inositol-requiring enzyme 1 (IRE1). Each of these proteins represents distinct pathways of the ER stress response.

(XBP1), a downstream target of ATF6, are up-regulated at mRNA level in SW620 cells (Table 1). XBP1 regulates a subset of ER-resident chaperones that are essential for protein folding, maturation, and degradation in the ER (34).

Cyclin D1 is significantly down-regulated both at mRNA and protein level (Table 1, Fig. 2B, C), probably mediated by phosphorylated eIF2 $\alpha$  that has been shown to attenuate cyclin D1 translation and cause cell-cycle arrest (G1 phase) in response to prolonged ER stress (15). mRNA for GADD34, a subunit in phosphorylated eIF2 $\alpha$  phosphatase, is up-regulated in SW620 cells, possibly explaining in part the decrease in phosphorylated eIF2 $\alpha$  at 12 h and later (Fig. 2A).

Induction of the UPR is initiated through dissociation of PERK from the ER-resident chaperone BiP/GRP78 that engages in numerous complexes (35). The protein level of BiP remained constant at all time points (data not shown). Treatment of SW620 cells with the ER stress inducers tunicamycin (1  $\mu$ g/ml) and thapsigargin (0.2  $\mu$ M) for 6 h, caused a marked down-regulation of cyclin D1 compared with control (results not shown). These results confirm that ER stress in SW620 cells leads to down-regulation of cyclin D1.

Induction of ER stress and UPR is followed by disruption of protein folding and destruction of defective proteins by ER-associated degradation. Several members of the molecular chaperone Hsp40, Hsp70, and Hsp90 families were up-regulated at the mRNA level (Table 1 and supplementary Table I). Hsp70 was also found to be up-regulated at the protein level (Fig. 2A).

Several transcripts belonging to the ubiquitin/proteasome system were up-regulated (Table 1 and supplementary Table I). The proteasome family of proteins is responsible for the degradation of damaged and short-lived proteins. In SW620, mRNA for 27 out of 34 subunits (present on the Human Genome Focus array) of the proteasome 26S were up-regulated. The proteasomal subunit proteasome 26S subunit, non-ATPase, 1 (PSMD1)/Rpn2 was significantly

increased relative to control at protein level (Fig. 2A). Also, the mRNA level of sequestosome 1 (SQSTM1), which serves as a storage place for ubiquitinated proteins in the cytoplasm, was up-regulated at all time points in SW620 cells (Table 1). These results support the view that the ER stress response initiated by DHA causes extensive changes in protein homeostasis in these cells.

We have previously shown that EPA has an antiproliferative effect on SW620 cells, although to a lesser extent than DHA, while OA has no effect (5). Key mediators of ER stress and UPR were also induced at protein level by EPA, but not OA, at equal molar concentrations (Fig. 3). DHA-treatment (70  $\mu$ M) of SW620 cells induced phosphorylation of eIF2 $\alpha$  already after 3 h (Fig. 2A), while a weaker response is observed after treatment with EPA (70  $\mu$ M) or half molar concentrations of DHA (35  $\mu$ M) first at 24 h (Fig. 3). A similar time- and concentration-dependent response is also observed for the induction of ATF4 (Fig. 3). Also, EPA (70  $\mu$ M) and DHA (35 and 70  $\mu$ M) reduced the level of cyclin D1 after 24 h (Fig. 2B, C and Fig. 3). After 6 h, only DHA (70  $\mu$ M) reduced the level of cyclin D1 significantly, whereas DHA (70  $\mu$ M) and EPA (70  $\mu$ M) both reduced cyclin D1 substantially and with comparable effects after 24 h. OA did not affect the proliferation of SW620 cells. However, OA reduced the level of cyclin D1 after 24 h, although to a much lesser extent (Fig. 3). This reflects the differences in the antiproliferative effect between the PUFAs observed earlier.

#### DHA induces antioxidant response

PUFAs are subject to lipid peroxidation, thus causing oxidative stress. Some cell lines that have weak antioxidant defense are highly sensitive to n-3 PUFAs for this reason (36). However, SW480 and SW620 cell lines display little sensitivity to lipid peroxidation products (5). Activated PERK phosphorylates nuclear factor (erythroid-derived 2)-like 2 (Nrf2) (up-regulated in SW620) (Table 1) that

TABLE 1. Functional categories of differentially expressed transcripts affected in SW620 cells treated with docosahexaenoic acid (DHA) (70  $\mu$ M) at time points indicated

Gene Symbol	Affymetrix ID	Refseq NCBI ID	Description	SW620 Fold Change		
				12 h	24 h	48 h
<b>ER Stress Response</b>						
ATF3	202672_s_at	NM_001030287 NM_001040619 NM_001674 NM_004024	Activating transcription factor 3	3.7	4.1	3.1
ATF4	200779_at	NM_001675 NM_182810	Activating transcription factor 4	2.1	2.0	1.6
ATF6	203952_at	NM_007348	Activating transcription factor 6	1.3	1.2	—
EIF2S1	201142_at	NM_004094	Eukaryotic translation initiation factor 2- $\alpha$	NC	NC	NC
GADD34	37028_at	NM_014330	Growth arrest and DNA-damage-inducible 34	6.3	3.9	—
NRF2	201146_at	NM_006164	Nuclear factor E2-related factor	2.0	1.8	—
PERK	218696_at	NM_004836	PKR-like ER kinase	1.4	2.0	—
VCP	208649_s_at	NM_007126	Valocin containing protein	1.9	1.6	—
XBP1	200670_at	NM_001079539 NM_005080	X-box binding protein 1	2.0	1.8	—
<b>Chaperones/Protein Folding/UPR Response</b>						
DNAJB1	200666_s_at	NM_006145	DnaJ homolog, subfamily B, member 1	8.0	4.1	—
HMOX1	203665_at	NM_002133	Heme oxygenase (decycling) 1	24.0	10.6	5.7
HSPA1A/B	200800_s_at	NM_005345 NM_005346	Heat shock 70 kDa protein 1A/B	17.8	9.8	5.1
HSPA1B	202581_at	NM_005346	Heat shock 70 kDa protein 1B	9.8	6.5	3.1
HSP47	207714_s_at	NM_001235	Heat shock protein 47	4.4	1.8	—
<b>Ubiquitine/Proteasome</b>						
PSMD1/RPN2	211198_s_at	NM_002807	Proteasome 26S subunit, non-ATPase, 1	2.2	2.2	—
SQSTM1	213112_s_at	NM_003900	Sequestosome 1	7.7	6.7	5.0
SQSTM1	201471_s_at	NM_003900	Sequestosome 1	6.7	7.3	3.9
<b>Ca<sup>2+</sup> Homeostasis</b>						
CAMLG	203538_at	NM_001745	Calcium modulating ligand	1.9	1.9	—
CAPN2	208683_at	NM_001748	Calpain 2, large subunit	1.3	1.8	1.4
CAPN7	203356_at	NM_014296	Calpain 7	—	1.5	—
IP3R1	203710_at	NM_002222	Inositol 1,4,5-triphosphate receptor, type 1	1.5	2.2	1.4
IP3R3	201189_s_at	NM_002224	Inositol 1,4,5-triphosphate receptor, type 3	—	—	1.3
<b>Antioxidants/Oxidative Stress</b>						
CAT	201432_at	NM_001752	Catalase	—	-1.4	—
GCLC	202922_at	NM_001498	Glutamate-cysteine ligase, catalytic subunit	1.6	1.3	—
GCLM	203925_at	NM_002061	Glutamate-cysteine ligase, modifier subunit	3.7	3.5	2.0
HMOX1	203665_at	NM_002133	Heme oxygenase (decycling) 1	24.0	10.6	5.7
SOD1	200642_at	NM_000454	Superoxide dismutase 1	1.5	1.6	—
TXNRD1	201266_at	NM_003330 NM_182729 NM_182742 NM_182743	Thioredoxin reductase 1	3.2	2.9	1.9
<b>Cell Cycle/Apoptosis</b>						
BAG3	217911_s_at	NM_004281	BCL2-associated athanogene 3	9.9	5.4	—
CASP4	209310_s_at	NM_001225 NM_033306 NM_033307	Caspase 4	1.6	2.9	—
CASP7	207181_s_at	NM_001227 NM_033338 NM_033339 NM_033340	Caspase 7	1.6	2.1	—
CCND1	208712_at	NM_053056	Cyclin D1	-1.7	-2.0	—
TRIB3	218145_at	NM_021158	Tribbles homolog 3 ( <i>Drosophila</i> )	7.4	6.5	3.3
<b>Cholesterol Biosynthesis, Uptake, Metabolism, and Transport</b>						
CAV1	203065_s_at	NM_001753	Caveolin 1, caveolae protein, 22 kDa	-1.5	-1.4	—
DHCR24	200862_at	NM_014762	24-dehydrocholesterol reductase	-1.6	-1.7	—
DHCR7	201791_s_at	NM_001360	7-dehydrocholesterol reductase	-1.6	-1.5	—
FDPS	201275_at	NM_002004	Farnesyl diphosphate synthase	-1.3	-1.2	—
HMGCR	202539_s_at	NM_000859	3-hydroxy-3-methylglutaryl-CoA reductase	NC	NC	NC
LDLR	202068_s_at	NM_000527	Low density lipoprotein receptor	2.4	2.4	—
LSS	202245_at	NM_002340	Lanosterol synthase	-1.3	—	—
NPC1	202679_at	NM_000271	Niemann-Pick disease, type C1	3.0	4.5	1.9
NPC2	200701_at	NM_006432	Niemann-Pick disease, type C2	—	1.5	1.5
OSBP	201800_s_at	NM_002556	Oxysterol binding protein	1.4	1.4	—
PMVK	203515_s_at	NM_006556	Phosphomevalonate kinase	-1.3	-1.8	—
SREBP2	201247_at	NM_004599	Sterol regulatory element binding protein 2	NC	NC	NC
TM7SF2	210130_s_at	NM_003273	Transmembrane 7 superfamily member 2	-1.4	-1.9	—
VLDLR	209822_s_at	NM_001018056 NM_003383	Very low density lipoprotein receptor	1.6	1.6	—

NC, no change; UPR, unfolded protein response.

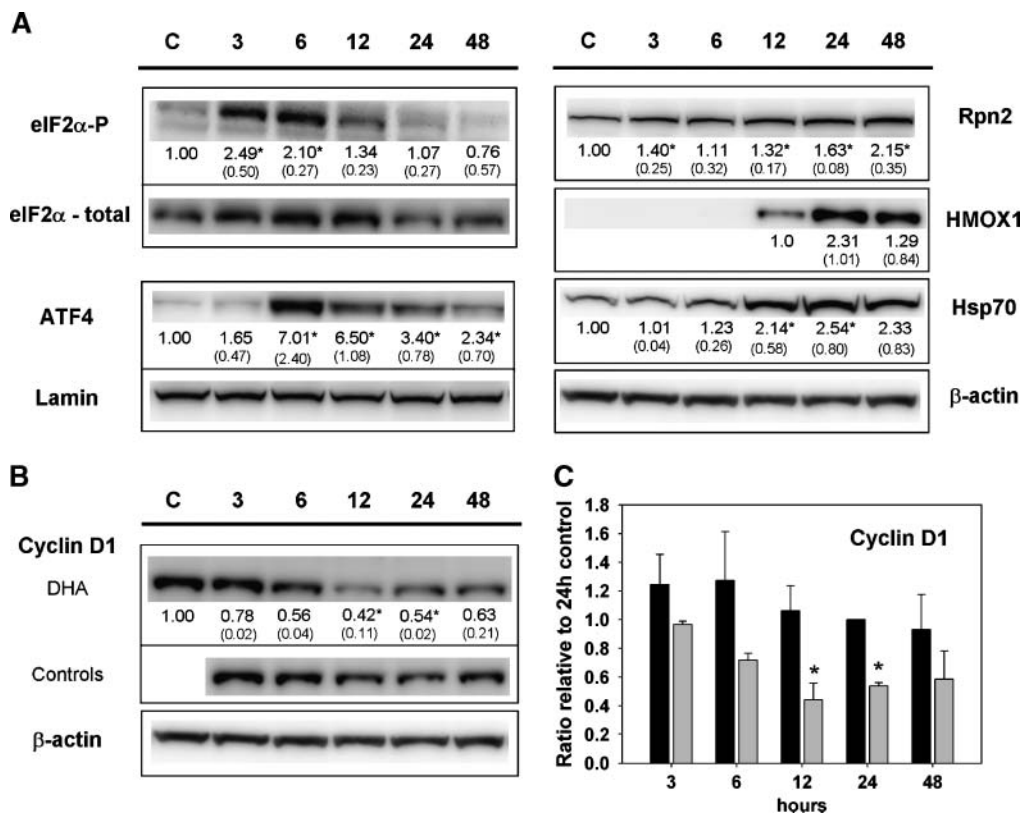


**Fig. 2.** Analysis of proteins involved in ER stress signaling and UPR. **A:** Western blot analysis of proteins involved in ER stress signaling and UPR from total cell extracts (except for ATF4: nuclear extracts; eIF2 $\alpha$ : cytoplasmic extracts) of SW620 cells treated with DHA for indicated time periods (h). Controls were harvested at all time points; only the 24 h control (C means control) is shown. **B:** Western blot analysis of cyclin D1 from total extracts of SW620 cells treated or not treated (controls) with DHA for the indicated time periods (h). **C:** Quantification of cyclin D1 Western blots in B [DHA treated cells (gray bars) compared with controls (black bars)]. Results were verified in three independent experiments; one representative blot is shown.  $\beta$ -actin (total extracts), lamin C (nuclear extracts), or total eIF2 $\alpha$  was used as a control for equal protein loading. The blots were quantified and protein band intensities normalized relative to loading control. The adjusted band intensities from the DHA and control membranes were then normalized relative to the 24 h control band, present at all membranes, to adjust for differences in signal intensities between the membranes. The numbers under the blots represent mean fold change (SD) of DHA samples relative to control at the indicated time points for three independent experiments. \* Significantly different from control (Student's *t*-test,  $P < 0.05$ ).

promotes transcription of genes involved in redox homeostasis, which contributes to survival of ER stress induced in mammalian cells. Oxidative stress-related genes that were found to be up-regulated in SW620 cells included thioredoxin reductase 1 (TXNRD1), superoxide dismutase 1 (SOD1), HMOX1, glutamate-cysteine ligase modifier (GCLM), and glutamate-cysteine ligase catalytic subunits, (GCLC) indicating a disturbance in the redox balance (Fig. 1 and Table 1). HMOX1, GCLM, and TXNRD1 are downstream targets of Nrf2 (14). HMOX1 displays a 24-fold induction at 12 h and is also strongly induced at the protein level (Fig. 2A and Table 1). HMOX1 catabolizes cellular heme to biliverdin, which is reduced to bilirubin, both being very potent cytoprotective antioxidants (37). However, knockdown of HMOX1 by siRNA did not result in increased DHA-sensitivity in SW620 cells (data not shown), supporting our previous findings that lipid peroxidation is not the key mediator of cytotoxicity.

#### Effect of DHA treatment on Ca<sup>2+</sup> homeostasis and genes involved in apoptosis

ER stress-induced depletion of Ca<sup>2+</sup> stores or dysregulation of Ca<sup>2+</sup> homeostasis may trigger apoptosis. We found that mRNA for a large number of genes involved in Ca<sup>2+</sup> homeostasis was changed, mostly up-regulated, after DHA treatment in SW620 cells. Thus, transcripts for the inositol 1,4,5-triphosphate receptors (IP3R1 and 3) were up-regulated, indicating a release of Ca<sup>2+</sup> regulated by these receptors (Table 1 and supplementary Table I). In agreement with this, treatment with DHA (70  $\mu$ M) for 12–48 h resulted in an increase in cytosolic Ca<sup>2+</sup> concentration (Fig. 4A). Cytosolic [Ca<sup>2+</sup>] is mainly regulated by means of transport across cell membranes (e.g., the plasma and ER membranes). Thapsigargin is a specific inhibitor of a Ca<sup>2+</sup> ATPase, which pumps Ca<sup>2+</sup> into ER. The rate of [Ca<sup>2+</sup>] increases in cytosol after addition of thapsigargin thus reflects Ca<sup>2+</sup> turnover in ER, the main intracellular

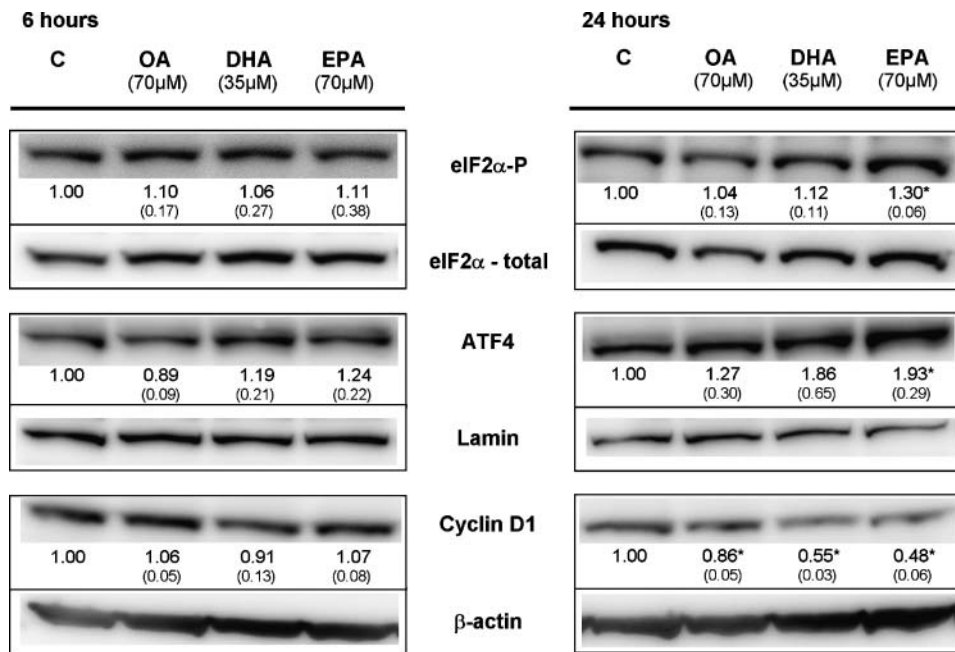


**Fig. 3.** ER stress signaling and UPR in response to n-3 polyunsaturated fatty acids (PUFAs) and oleic acid (OA). Western blot analysis of proteins involved in ER stress signaling and UPR (ATF4: nuclear extracts; cyclin D1, eIF2α: cytoplasmic extracts) in SW620 cells treated with complete growth medium supplemented with either OA (70 μM), DHA (35 μM), eicosapentaenoic acid (EPA, 70μM), or ethanol (control media, C) for 6 and 24 h. β-actin (cytoplasmic extracts), lamin C (nuclear extracts), or total eIF2α was used as a control for equal protein loading. One representative blot is shown. The blots were quantified and intensities normalized relative to loading control. The numbers under the blots represent mean fold change (SD) relative to control for three independent experiments. \* Significantly different from control (Student's *t*-test, *P* < 0.05).

Ca<sup>2+</sup> store. In SW620 this effect was apparent first after 48 h DHA incubation (average [Ca<sup>2+</sup>] increase 267nM vs. 187nM in control). The time course of these registrations is shown in Fig. 4B.

A Ca<sup>2+</sup> signal after agonist-binding to a G protein coupled receptor often displays two phases: an initial peak response, which is due to release from intracellular stores; and a prolonged phase, which is attributable to Ca<sup>2+</sup> entry through the plasma membrane due to emptying of intracellular Ca<sup>2+</sup> stores ("capacitative" or store operated Ca<sup>2+</sup> influx). This Ca<sup>2+</sup> entry is abolished when free extracellular [Ca<sup>2+</sup>] is chelated by ethylene glycol tetraacetic acid (EGTA). We find that ATP is an agonist that releases a two-phasic Ca<sup>2+</sup> signal in most SW620 cells. Incubation with DHA for 12 h and more seemed to accentuate the second phase Ca<sup>2+</sup> elevation in SW620 cells (Fig. 4C, Table 2), whereas the first peak response was virtually unchanged. The time course of the registrations from ATP-stimulated SW620 cells are shown in Fig. 4C. When EGTA was added to SW620 cells treated with DHA for 24 h and then stimulated with ATP, we found that the second phase Ca<sup>2+</sup> elevation was abolished (Fig. 4D, Table 3). The elevation in prolonged Ca<sup>2+</sup> signal in DHA-treated cells after ATP stimulation can therefore be ascribed to Ca<sup>2+</sup> entry, probably of the capacitative type.

Disturbances in the Ca<sup>2+</sup> pool of ER activate calpain in the cytosol, which then converts ER-localized procaspase 12 to caspase 12 (38). Calpain 7 and a large subunit of

calpain 2 as well as the ER stress-related caspases (caspase 4 and 7) were up-regulated in SW620 cells (Table 1). The proapoptotic members of the Bcl-2 family, BAD and BIK, were down-regulated, while BID was up-regulated (SW620). BCL2-associated athanogene 3 (BAG3), known to participate in regulation of apoptosis, was up-regulated 9.9-fold in SW620 cells after 12 h incubation with DHA. Also, the proapoptotic factor Tribbles homolog 3 (TRIB3), known to be induced by ER stress through the PERK-ATF4-CHOP pathway, was up-regulated at all time points (Table 1) (39). The protein level of active caspase 7 was found to increase with time in SW480 cells, while not detected in SW620 cells (data not shown).

#### Effect of DHA on cellular cholesterol and cholesterol metabolism

We have previously shown that treatment of SW480 and SW620 with DHA leads to accumulation of numerous large lipid droplets, mainly containing triglycerides in SW480 and cholesteryl esters in SW620 (5). However, an increase in cholesteryl esters was also seen in SW480. The formation of lipid droplets is probably induced by DHA, since they are highly enriched in this PUFA. To examine whether this accumulation of esterified cholesterol was compensated for by increased total cholesterol levels, we measured cellular cholesterol content after DHA treatment. No significant differences in total cholesterol were found at 3–24 h when comparing control and DHA-treated cells



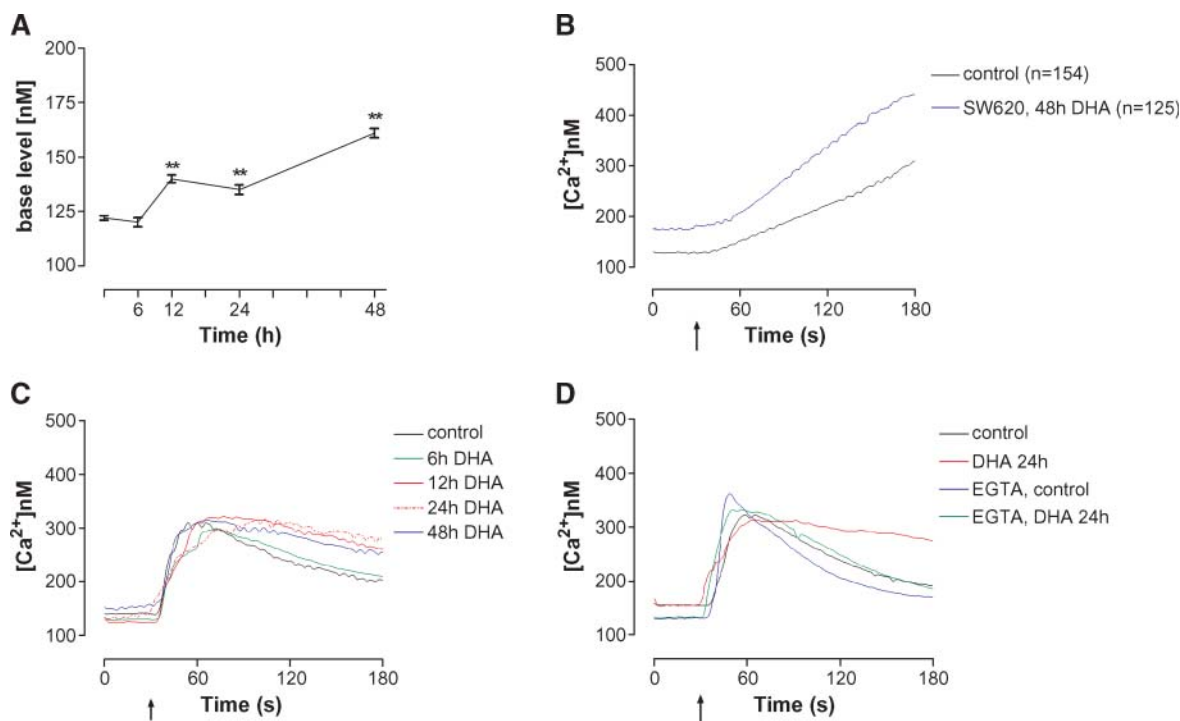


**Fig. 4.** Cytosolic  $\text{Ca}^{2+}$  release after DHA treatment. Registrations of cytosolic  $\text{Ca}^{2+}$  in DHA-treated SW620 cells. **A:** DHA treatment increases the basic cytosolic  $\text{Ca}^{2+}$  level in SW620 cells. SW620 cells were incubated with DHA ( $70 \mu\text{M}$ ) for various time periods as indicated. Average  $\text{Ca}^{2+}$  concentrations in 196–324 cells are shown. Bars indicate SEM values. The average basic cytosolic  $\text{Ca}^{2+}$  level from each time period was tested against time 0. Statistically significant difference from control (no treatment): \*\*  $P < 0.01$ . **B:** DHA treatment affects the thapsigargin-inhibited  $\text{Ca}^{2+}$  transport. SW620 cells were incubated with DHA ( $70 \mu\text{M}$ ) for 48 h as indicated. After 30 s of  $[\text{Ca}^{2+}]_i$  registration thapsigargin ( $5 \mu\text{M}$ ) (Sigma-Aldrich) or vehicle was added (arrow). Average registrations from all cells are shown since virtually all cells responded. Cytosolic  $[\text{Ca}^{2+}]_i$  at the end of the registration (180 s) in DHA-treated cells was statistically significant different from control ( $P < 0.05$ ). **C:** ATP stimulation causes a prolonged  $\text{Ca}^{2+}$  signal in DHA-treated cells. SW620 cells were incubated with DHA ( $70 \mu\text{M}$ ) for various time periods as indicated. After 30 s of  $[\text{Ca}^{2+}]_i$  registration ATP ( $1 \mu\text{M}$ ) was added (arrow). Average registrations from responding cells are shown. **D:** Removal of extracellular  $\text{Ca}^{2+}$  with ethylene glycol tetraacetic acid (EGTA) abolishes the prolonged ATP response in DHA-treated cells. SW620 cells were incubated with DHA ( $70 \mu\text{M}$ ) for 24 h. The cells were incubated in a 10 mM HEPES buffer without  $\text{Ca}^{2+}$ , but with 0.1 mM EGTA or in a 10 mM HEPES buffer containing 1.2 mM  $\text{Ca}^{2+}$  for 10 min before registration. After 30 s of  $[\text{Ca}^{2+}]_i$  registration, ATP ( $1 \mu\text{M}$ ) was added (arrow). Average registrations from responding cells are shown.

(data not shown). A slight, but significant increase in total cholesterol levels in DHA-treated cells was observed at 48 h ( $31.28 \pm 1.29$  (control) vs.  $38.75 \pm 3.39 \mu\text{g}$  cholesterol/mg protein,  $P < 0.05$ ). These results may indicate that cholesterol available for organelles is reduced due to deposition in lipid droplets.

From the gene expression data, it was apparent that several genes encoding proteins involved in cholesterol biosynthesis were down-regulated at the mRNA level in DHA-treated SW620 cells (Table 1). These include 7- and 24-dehydrocholesterol reductase (DHCR7, DHCR24), farnesyl diphosphate synthase (FDPS), phosphomevalonate

**TABLE 2.**  $\text{Ca}^{2+}$  registrations in SW620 cells pretreated with DHA ( $70 \mu\text{M}$ ) at time points indicated: SW620 cells stimulated with ATP,  $1 \mu\text{M}$

Pretreatment	# Cells (Responding Cells, %)	Maximal $[\text{Ca}^{2+}]_i$ Increase, nM	Decline of the Response
None (control)	120 (56)	190 ( $\pm 13.2$ )	1.64 ( $\pm 0.06$ )
DHA 6 h	110 (53)	196 ( $\pm 10.8$ )	1.66 ( $\pm 0.16$ )
DHA 12 h	107 (55)	226 ( $\pm 15.9$ ) <sup>a</sup>	1.39 ( $\pm 0.06$ ) <sup>a</sup>
DHA 24 h	94 (51)	201 ( $\pm 18.4$ )	1.27 ( $\pm 0.09$ ) <sup>b</sup>
DHA 48 h	97 (45)	198 ( $\pm 21.1$ )	1.23 ( $\pm 0.04$ ) <sup>b</sup>

After 30 s of  $[\text{Ca}^{2+}]_i$  registration ATP ( $1 \mu\text{M}$ ) (Sigma-Aldrich) or vehicle was added. Maximal  $[\text{Ca}^{2+}]_i$  increase is calculated as difference between baseline and peak  $[\text{Ca}^{2+}]_i$  in the responding cells. The decline of the response is quantified as the ratio between peak  $[\text{Ca}^{2+}]_i$  and  $[\text{Ca}^{2+}]_i$  at the end of the registration (180 s). Registrations are depicted in Fig. 4C. The data are presented as means with standard errors ( $\pm$  SEM).

<sup>a</sup> Statistically significant difference from control ( $P < 0.05$ ).

<sup>b</sup> Statistically significant difference from control ( $P < 0.01$ ).



TABLE 3.  $\text{Ca}^{2+}$  registrations in SW620 cells pretreated with DHA (70  $\mu\text{M}$ ) at time points indicated: SW620 cells stimulated with ATP, 1 $\mu\text{M}$

Pretreatment	# Cells	Baseline $[\text{Ca}^{2+}]$ , nM	Maximal $[\text{Ca}^{2+}]$ Increase, nM	Decline of the Response
None (control)	103	123 ( $\pm$ 4.1)	247 ( $\pm$ 10.6)	2.07 ( $\pm$ 0.09)
DHA 24 h	85	141 ( $\pm$ 4.7) <sup>a</sup>	238 ( $\pm$ 14.1)	1.61 ( $\pm$ 0.07) <sup>a</sup>
2. EGTA	81	103 ( $\pm$ 3.7) <sup>a</sup>	259 ( $\pm$ 18.2)	2.51 ( $\pm$ 0.14) <sup>a</sup>
EGTA, DHA 24 h	73	105 ( $\pm$ 3.8) <sup>a,b</sup>	227 ( $\pm$ 17.3)	2.11 ( $\pm$ 0.12) <sup>a,b</sup>

EGTA, ethylene glycol tetraacetic acid. After 30 s of  $[\text{Ca}^{2+}]$  registration ATP (1 $\mu\text{M}$ ) (Sigma-Aldrich) or vehicle was added. Maximal  $[\text{Ca}^{2+}]$  increase is calculated as difference between baseline and peak  $[\text{Ca}^{2+}]$  in the responding cells. The decline of the response is quantified as the ratio between peak  $[\text{Ca}^{2+}]$  and  $[\text{Ca}^{2+}]$  at the end of the registration (180 s). Registrations are depicted in Fig. 4D. The data are presented as means with standard errors ( $\pm$  SEM).

<sup>a</sup>Significantly different from control ( $P < 0.05$ ).

<sup>b</sup>Significantly different from DHA 24 h ( $\pm$  EGTA) ( $P < 0.001$ ).

kinase (PMVK), 3 $\beta$ -hydroxysterol  $\Delta$ 14-reductase (TM7SF2) (12, 24 h), and lanosterol synthase (LSS) (12 h). However, some transcripts involved in cholesterol uptake and intracellular cholesterol transport, such as low and very low density lipoprotein receptor (LDLR, VLDLR), the Niemann-Pick

C1 protein (NPC1), NPC2, and the oxysterol binding protein (OSBP), were found to be up-regulated in SW620 cells after DHA-treatment (Table 1). NPC1 protein levels were in addition analyzed by Western blot and were increased in DHA-treated cells compared with control at 24 h (Fig. 5A).

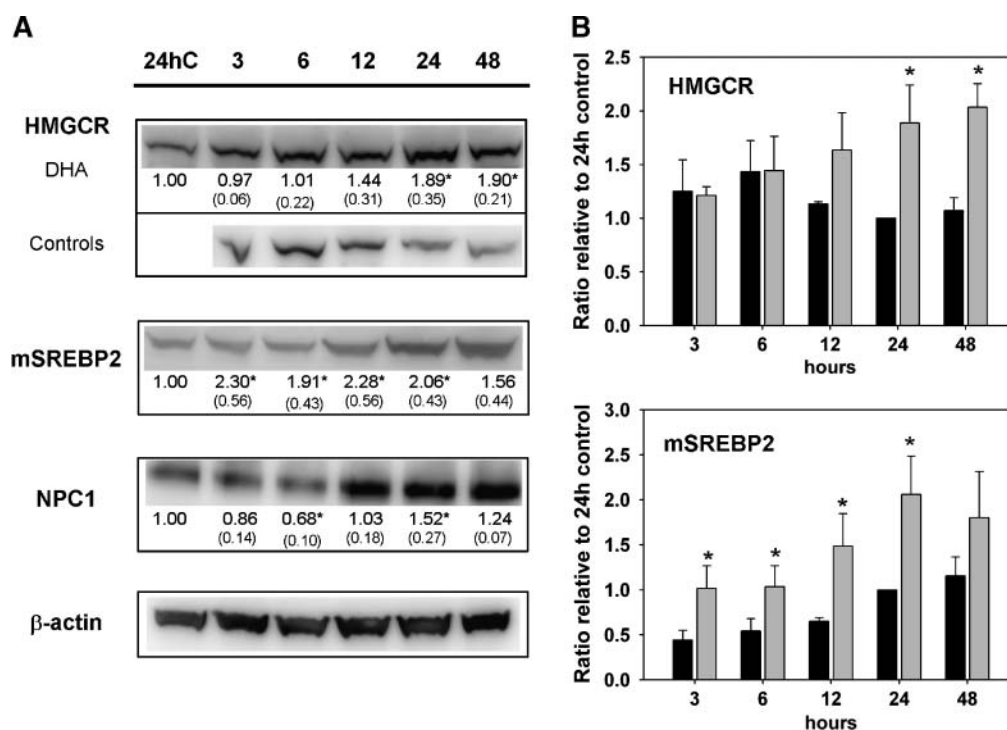


**Fig. 5.** Changes in cholesterol metabolism induced by DHA. A: Western blot analysis of HMGCR, mSREBP2, and NPC1 protein levels in total protein extracts from SW620 cells treated with DHA for the indicated time periods (h). Controls were harvested at all time points; only 24 h control is shown for mSREBP2 and NPC1. For HMGCR, controls are shown for all time points.  $\beta$ -actin was used as a control for equal protein loading. One blot, representing three independent experiments, is shown. The blots were quantified and protein band intensities normalized relative loading control. The actin adjusted band intensities from the DHA and control membranes were further normalized relative to the 24 h control band, present at all membranes, to adjust for differences in signal intensities between the membranes. The numbers under the blots represent mean fold change (with SD) of DHA samples relative to control at indicated time points for three independent experiments. \* Significantly different from control (Student's  $t$ -test,  $P < 0.05$ ). B: Alterations in HMGCR and mSREBP2 protein levels in control (baseline) and DHA treated cells at the indicated time periods. The plots show the mean value of the actin adjusted band intensities normalized relative to the 24 h control band for DHA treated cells (gray bars) and control cells (black bars). The data represent the mean and SD of three independent experiments. \* Significantly different from control (Student's  $t$ -test,  $P < 0.05$ ).

Since several of the differentially expressed transcripts listed above are regulated by sterol regulatory element binding protein 2 (SREBP2), the protein levels of mSREBP2 (mature) and pSREBP2 (precursor) were analyzed by Western blot. An increase in mSREBP2 levels was observed in control and DHA-treated cells over the time period assayed, but DHA-treated cells displayed higher levels of mSREBP2 compared with control cells at all time points (Fig. 5A, B). The level of pSREBP2 was unchanged in SW620 control cells at all time points, while a slight decrease was observed after 48 h treatment with DHA (data not shown). We also analyzed the level of the rate-limiting enzyme in cholesterol biosynthesis, 3-hydroxy-3-methylglutaryl-CoA reductase (HMGCR) by Western blot after DHA treatment. The protein levels of HMGCR in DHA-treated and control cells were similar at 3 and 6 h. At 12–48 h, the HMGCR protein levels were reduced in controls, while the protein level in DHA-treated cells increased slightly (Fig. 5A, B).

To investigate de novo synthesis of cholesterol in DHA-treated cells, the incorporation of  $^{14}\text{C}$ -acetate into cholesterol and cholesteryl esters was measured after treating the cells with DHA for 24 h. The amount of  $^{14}\text{C}$ -acetate incorporated into cholesterol in DHA treated cells was slightly, but significantly lower relative to control at 4 h; a similar trend, although not significant was seen after 6 h (Fig. 6). The amount of  $^{14}\text{C}$ -acetate incorporated into cholesteryl esters in DHA treated cells was reduced by approximately 60% relative to control at both time points (Fig. 6).

## DISCUSSION

Exploring how dietary factors interact with and modulate signaling pathways to promote or counteract cancer development and progression constitutes a major challenge. The purpose of the present study was to examine whether n-3 PUFAs like DHA exert their cytotoxicity by

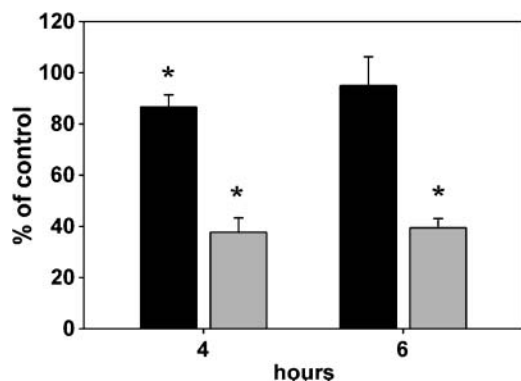


**Fig. 6.** Effect of DHA on incorporation of  $^{14}\text{C}$ -acetate into cholesterol and cholesteryl esters. Amount of  $^{14}\text{C}$ -acetate (% of control) incorporated in cholesterol (black bars) and cholesteryl esters (gray bars) in SW620 cells treated with DHA for 24 h, and further coincubated with DHA and  $^{14}\text{C}$ -acetate for 4 and 6 h. The mean and  $\pm$  SD from (4 h,  $n = 3$ ; 6 h,  $n = 2$ ) independent experiments is displayed. \* Significantly different from control (Student's  $t$ -test,  $P < 0.05$ ).

changing gene expression patterns and signaling pathways regulating cell growth. We found that ER stress is established already after 3 h treatment with DHA, as demonstrated by increased levels of phosphorylated eIF2 $\alpha$ , a hallmark of ER stress. Phosphorylation of eIF2 $\alpha$  adapts cells to various conditions of stress by attenuation of protein synthesis. We found that the n-3 PUFAs DHA and EPA, but not OA, cause phosphorylation of eIF2 $\alpha$ , thereby generally inhibiting translation initiation. This is in agreement with previous results showing that inhibition of translation initiation mediates the antiproliferative action of EPA in NIH 3T3 cells by decreased levels of cyclin D1 (40). Increased expression of genes downstream of phosphorylated eIF2 $\alpha$  is mediated through induction of the transcription factor ATF4 (14). Genes with ATF4 binding sites are involved in restoring ER homeostasis in response to various stresses (41). Several downstream targets of ATF4 are affected at the mRNA and protein level in our study, indicating that ER stress induced by DHA in SW620 cells is mediated through the ER-localized PERK pathway. Induction of the UPR is initiated by dissociation of PERK from the ER-resident chaperone BiP. However, the protein level of BiP remained constant at all time points. Pimpl et al. (42) have reported that transcriptional induction of *BiP* rarely leads to increased protein levels of BiP/GRP78, this being due to increased turnover.

UPR is activated to restore cellular homeostasis and induces transcription of genes encoding proteins that mediate ER-associated degradation in response to prolonged ER stress. A large number of 20S and 26S proteasomal subunits were up-regulated in SW620 cells. The proteasome plays a central role in proteolysis of ubiquitinated proteins and are responsible for cleaving many regulatory proteins, like cyclins and members of the NF $\kappa$ B family (43). Prolonged ER stress may cause induction of apoptosis. We show that even though the ER stress-related caspases 4 and 7 are up-regulated in DHA-treated SW620 cells, active caspase 7 is not detectable. On the other hand, active caspase 7 was detected in SW480 cells (data not shown). Chen and Istfan (44) have studied the apoptotic response to DHA in several cell lines, among these SW480 and SW620. A DNA ladder was observed after incubation with DHA (150  $\mu\text{M}$ ) for 24 h in SW480, but not in SW620 cells; this is in accordance with our results. Previously, we were not able to detect apoptosis by the TUNEL-assay in either SW480 or SW620 (5). This may indicate that the survival threshold is not exceeded in these cells within the time period assayed and concentration used.

ER is the principal site for protein synthesis and folding,  $\text{Ca}^{2+}$  storage and signaling, as well as biosynthesis of fatty acids and cholesterol. Any perturbation that interferes with these activities promotes ER stress and initiates the UPR. We found that DHA treatment mobilizes  $\text{Ca}^{2+}$  from ER into the cytosol, in agreement with previous results investigating the effects of n-3 and n-6 PUFAs (40, 45–47), but the mechanism is not known. Our results indicate that calcium release induced by DHA may be linked to induction of ER stress. A redistribution of cholesterol from intracellular regulatory compartments like ER to DHA-cholesteryl

ester-enriched lipid droplets (5), causing functional depletion of cholesterol in the ER could potentially lead to ER stress and Ca<sup>2+</sup> mobilization, since total cholesterol is not increased (this work). Harding et al. (21) have shown that compounds that deplete cellular cholesterol stores activate an integrated stress response (ISR) by promoting ER stress.

The observed stabilization of HMGCR, the rate limiting enzyme in cholesterol biosynthesis, and the increased level of mSREBP2 observed in DHA-treated SW620 cells, indicate an increased cellular need for de novo synthesized cholesterol during DHA treatment. Surprisingly, both increased and decreased expression of several SREBP2 target genes is observed in SW620, despite an increase in the active transcription factor. Inhibition of transcription of SREBP2 target genes has previously been associated with ER stress-induced activation and cleavage of ATF6, and is mediated by interaction of the two transcription factors in the nucleus (48). Reduced expression of SREBP2 target genes may result in a decreased ability of the cells to synthesize new cholesterol, in spite of activated SREBP2. In line with this, we show that DHA promotes a reduced de novo synthesis of cholesterol. Surprisingly, we also find a reduced incorporation of newly synthesized cholesterol into cholesteryl esters (this work), despite the previous observed accumulation of cholesteryl esters in SW620 cells treated with DHA (5). This might possibly result from reduced turnover of DHA-enriched cholesteryl esters in droplets resulting in accumulation in spite of reduced synthesis.

Recently, a link between molecular chaperones, heat stress, and cholesterol synthesis was demonstrated (49). In this work, the chaperone DnaJA4 (DnaJ/Hsp40) was identified as a novel SREBP target gene that can be turned on under conditions of low sterol availability and heat shock. They postulated that SREBP-regulated chaperones may function as effectors linking heat-shock response and the maintenance of membrane components. Also, Lee and Ye (18) have shown that both hypotonic conditions and thapsigargin induced ER stress in CHO-7 cells leads to activation of SREBP2, while no increase in cholesterol synthesis was observed.

The reasons why SREBP2 target genes are regulated differently, and consequences thereof, remain to be investigated in our system.

Up-regulation of transcripts involved in cellular uptake and intracellular transport of cholesterol, like LDLR, VLDLR, NPC1/NPC2, and OSBP in SW620 cells treated with DHA, also suggests an increased demand for intracellular cholesterol. A recent report indicates that DHA treatment inhibits transport of exogenous cholesterol from the plasma membrane to the ER by an unknown mechanism in CaCo2 colon cancer cells (50). In addition, a study on a panel of colon carcinoma cell lines revealed a deficiency of the LDLR in SW480 cells, indicating a dependency on endogenous cholesterol biosynthesis (51). This would probably also apply to the SW620 cell line, which is established from a metastasis derived from the primary SW480 tumor. Reduced de novo cholesterol synthesis and inhibition of transport of exogenous cholesterol to the ER

pool, in combination with increased cholesterol esterification as observed earlier, may lead to depletion of cholesterol in the ER. This may be an important factor contributing to the observed prolonged ER stress that may cause growth inhibition and eventually cell death.

In vitro studies suggest that pharmacological activation of the UPR can alter the sensitivity of tumor cells to chemotherapeutic agents (52). Understanding how common dietary chemicals like DHA affect gene expression and signaling pathways in tumor cells may reveal possible treatment strategies that may be targeted and possibly enhance the impact of conventional therapy.

Technical assistance from Beate Buland and Jens Erik Slagsvold is highly appreciated. We are sincerely grateful for the generous financial support given to the project in remembrance of Egon Leren.

## REFERENCES

1. von Schacky, C., and W. S. Harris. 2007. Cardiovascular benefits of omega-3 fatty acids. *Cardiovasc. Res.* **73**: 310–315.
2. Stamp, L. K., M. J. James, and L. G. Cleland. 2005. Diet and rheumatoid arthritis: a review of the literature. *Semin. Arthritis Rheum.* **35**: 77–94.
3. Terry, P. D., T. E. Rohan, and A. Wolk. 2003. Intakes of fish and marine fatty acids and the risks of cancers of the breast and prostate and of other hormone-related cancers: a review of the epidemiologic evidence. *Am. J. Clin. Nutr.* **77**: 532–543.
4. Kato, T., R. L. Hancock, H. Mohammadpour, B. McGregor, P. Manalo, S. Khaiboullina, M. R. Hall, L. Pardini, and R. S. Pardini. 2002. Influence of omega-3 fatty acids on the growth of human colon carcinoma in nude mice. *Cancer Lett.* **187**: 169–177.
5. Schönberg, S. A., A. G. Lundemo, T. Fladvad, K. Holmgren, H. Bremseth, A. Nilsen, O. Gederaas, K. E. Tvedt, K. W. Egeberg, and H. E. Krokan. 2006. Closely related colon cancer cell lines display different sensitivity to polyunsaturated fatty acids, accumulate different lipid classes and downregulate sterol regulatory element-binding protein 1. *FEBS J.* **273**: 2749–2765.
6. Das, U. N. 1999. Essential fatty acids and their metabolites and cancer. *Nutrition.* **15**: 239–240.
7. Das, U. N. 1999. Essential fatty acids, lipid peroxidation and apoptosis. *Prostaglandins Leukot. Essent. Fatty Acids.* **61**: 157–163.
8. Stoll, B. A. 2002. N-3 fatty acids and lipid peroxidation in breast cancer inhibition. *Br. J. Nutr.* **87**: 193–198.
9. Finstad, H. S., M. C. Myhrstad, H. Heimli, J. Lomo, H. K. Blomhoff, S. O. Kolset, and C. A. Drevon. 1998. Multiplication and death-type of leukemia cell lines exposed to very long-chain polyunsaturated fatty acids. *Leukemia.* **12**: 921–929.
10. Finstad, H. S., H. Dyrendal, M. C. Myhrstad, H. Heimli, and C. A. Drevon. 2000. Uptake and activation of eicosapentaenoic acid are related to accumulation of triacylglycerol in Ramos cells dying from apoptosis. *J. Lipid Res.* **41**: 554–563.
11. Sampath, H., and J. M. Ntambi. 2005. Polyunsaturated fatty acid regulation of genes of lipid metabolism. *Annu. Rev. Nutr.* **25**: 317–340.
12. Narayanan, B. A., N. K. Narayanan, B. Simi, and B. S. Reddy. 2003. Modulation of inducible nitric oxide synthase and related proinflammatory genes by the omega-3 fatty acid docosahexaenoic acid in human colon cancer cells. *Cancer Res.* **63**: 972–979.
13. Wahle, K. W., D. Rotondo, and S. D. Heys. 2003. Polyunsaturated fatty acids and gene expression in mammalian systems. *Proc. Nutr. Soc.* **62**: 349–360.
14. Schroder, M. 2007. Endoplasmic reticulum stress responses. *Cell. Mol. Life Sci.* **65**: 862–894.
15. Schroder, M., and R. J. Kaufman. 2005. ER stress and the unfolded protein response. *Mutat. Res.* **569**: 29–63.
16. Momoi, T. 2004. Caspases involved in ER stress-mediated cell death. *J. Chem. Neuroanat.* **28**: 101–105.

17. Ye, J., R. B. Rawson, R. Komuro, X. Chen, U. P. Dave, R. Prywes, M. S. Brown, and J. L. Goldstein. 2000. ER stress induces cleavage of membrane-bound ATF6 by the same proteases that process SREBPs. *Mol. Cell*. **6**: 1355–1364.
18. Lee, J. N., and J. Ye. 2004. Proteolytic activation of sterol regulatory element-binding protein-2. *Int. J. Biochem. Cell Biol.* **39**: 1843–1851.
19. Colgan, S. M., D. Tang, G. H. Werstuck, and R. C. Austin. 2007. Endoplasmic reticulum stress causes the activation of sterol regulatory element binding protein-2. *Int. J. Biochem. Cell Biol.* **39**: 1843–1851.
20. Feng, B., P. M. Yao, Y. Li, C. M. Devlin, D. Zhang, H. P. Harding, M. Sweeney, J. X. Rong, G. Kuriakose, E. A. Fisher, et al. 2003. The endoplasmic reticulum is the site of cholesterol-induced cytotoxicity in macrophages. *Nat. Cell Biol.* **5**: 781–792.
21. Harding, H. P., Y. Zhang, S. Khersonsky, S. Marciniak, D. Scheuner, R. J. Kaufman, N. Javitt, Y. T. Chang, and D. Ron. 2005. Bioactive small molecules reveal antagonism between the integrated stress response and sterol-regulated gene expression. *Cell Metab.* **2**: 361–371.
22. Irizarry, R. A., B. M. Bolstad, F. Collin, L. M. Cope, B. Hobbs, and T. P. Speed. 2003. Summaries of Affymetrix GeneChip probe level data. *Nucleic Acids Res.* **31**: e15.
23. Bolstad, B. M., R. A. Irizarry, M. Astrand, and T. P. Speed. 2003. A comparison of normalization methods for high density oligonucleotide array data based on variance and bias. *Bioinformatics.* **19**: 185–193.
24. Smyth, G. K. 2004. Linear models and empirical bayes methods for assessing differential expression in microarray experiments. *Stat. Appl. Genet. Mol. Biol.* **3**: 1–27.
25. Benjamini, Y., and Y. Hochberg. 1995. Controlling the false discovery rate—a practical and powerful approach to multiple testing. *J. Royal Statistical Soc. B.* **57**: 289–300.
26. Langaas, M., B. H. Lindqvist, and E. Ferkingstad. 2005. Estimating the proportion of true null hypotheses, with application to DNA microarray data. *J. Royal Statistical Soc. B.* **67**: 555–572.
27. R Development Core Team. 2004. R: A language and environment for statistical computing. Accessed July 28, 2008 at <http://www.R-project.org>. Vol. 2005.
28. Gentleman, R. C., V. J. Carey, D. M. Bates, B. Bolstad, M. Dettling, S. Dudoit, B. Ellis, L. Gautier, Y. Ge, J. Gentry, et al. 2004. Bioconductor: open software development for computational biology and bioinformatics. *Genome Biol.* **5**: 1–16.
29. Rottingen, J. A., T. Enden, E. Camerer, J. G. Iversen, and H. Prydz. 1995. Binding of human factor VIIa to tissue factor induces cytosolic Ca<sup>2+</sup> signals in J82 cells, transfected COS-1 cells, Madin-Darby canine kidney cells and in human endothelial cells induced to synthesize tissue factor. *J. Biol. Chem.* **270**: 4650–4660.
30. Rotnes, J. S., and J. G. Iversen. 1992. Thapsigargin reveals evidence for fMLP-insensitive calcium pools in human leukocytes. *Cell Calcium.* **13**: 487–500.
31. Grynkiewicz, G., M. Poenie, and R. Y. Tsien. 1985. A new generation of Ca<sup>2+</sup> indicators with greatly improved fluorescence properties. *J. Biol. Chem.* **260**: 3440–3450.
32. Rotnes, J. S., and J. A. Rottingen. 1994. Quantitative analysis of cytosolic free calcium oscillations in neutrophils by mathematical modelling. *Cell Calcium.* **15**: 467–482.
33. Bligh, E. G., and W. J. Dyer. 1959. A rapid method of total lipid extraction and purification. *Can. J. Biochem. Physiol.* **37**: 911–917.
34. Okada, T., H. Yoshida, R. Akazawa, M. Negishi, and K. Mori. 2002. Distinct roles of activating transcription factor 6 (ATF6) and double-stranded RNA-activated protein kinase-like endoplasmic reticulum kinase (PERK) in transcription during the mammalian unfolded protein response. *Biochem. J.* **366**: 585–594.
35. Kleizen, B., and I. Braakman. 2004. Protein folding and quality control in the endoplasmic reticulum. *Curr. Opin. Cell Biol.* **16**: 343–349.
36. Schonberg, S. A., P. K. Rudra, R. Noding, F. Skorpen, K. S. Bjerve, and H. E. Krokan. 1997. Evidence that changes in Se-glutathione peroxidase levels affect the sensitivity of human tumour cell lines to n-3 fatty acids. *Carcinogenesis.* **18**: 1897–1904.
37. Stocker, R. 2004. Antioxidant activities of bile pigments. *Antioxid. Redox Signal.* **6**: 841–849.
38. Orrenius, S., B. Zhivotovsky, and P. Nicotera. 2003. Regulation of cell death: the calcium-apoptosis link. *Nat. Rev. Mol. Cell Biol.* **4**: 552–565.
39. Corcoran, C. A., X. Luo, Q. He, C. Jiang, Y. Huang, and M. S. Sheikh. 2005. Genotoxic and endoplasmic reticulum stresses differentially regulate TRB3 expression. *Cancer Biol. Ther.* **4**: 1063–1067.
40. Palakurthi, S. S., R. Fluckiger, H. Aktas, A. K. Changolkar, A. Shahsafaei, S. Harneit, E. Kilic, and J. A. Halperin. 2000. Inhibition of translation initiation mediates the anticancer effect of the n-3 polyunsaturated fatty acid eicosapentaenoic acid. *Cancer Res.* **60**: 2919–2925.
41. Harding, H. P., Y. Zhang, H. Zeng, I. Novoa, P. D. Lu, M. Calfon, N. Sadri, C. Yun, B. Popko, R. Paules, et al. 2003. An integrated stress response regulates amino acid metabolism and resistance to oxidative stress. *Mol. Cell.* **11**: 619–633.
42. Pimpl, P., J. P. Taylor, C. Snowden, S. Hillmer, D. G. Robinson, and J. Denecke. 2006. Golgi-mediated vacuolar sorting of the endoplasmic reticulum chaperone BiP may play an active role in quality control within the secretory pathway. *Plant Cell.* **18**: 198–211.
43. Olivier, S., P. Robe, and V. Bours. 2006. Can NF-kappaB be a target for novel and efficient anti-cancer agents? *Biochem. Pharmacol.* **72**: 1054–1068.
44. Chen, Z. Y., and N. W. Istfan. 2000. Docosahexaenoic acid is a potent inducer of apoptosis in HT-29 colon cancer cells. *Prostaglandins Leukot. Essent. Fatty Acids.* **63**: 301–308.
45. Chow, S. C., and M. Jondal. 1990. Polyunsaturated free fatty acids stimulate an increase in cytosolic Ca<sup>2+</sup> by mobilizing the inositol 1,4,5-trisphosphate-sensitive Ca<sup>2+</sup> pool in T cells through a mechanism independent of phosphoinositide turnover. *J. Biol. Chem.* **265**: 902–907.
46. Aktas, H., and J. A. Halperin. 2004. Translational regulation of gene expression by omega-3 fatty acids. *J. Nutr.* **134**: 2487S–2491S.
47. Kolar, S. S., R. Barhoumi, J. R. Lupton, and R. S. Chapkin. 2007. Docosahexaenoic acid and butyrate synergistically induce colonocyte apoptosis by enhancing mitochondrial Ca<sup>2+</sup> accumulation. *Cancer Res.* **67**: 5561–5568.
48. Zeng, L., M. Lu, K. Mori, S. Luo, A. S. Lee, Y. Zhu, and J. Y. Shyy. 2004. ATF6 modulates SREBP2-mediated lipogenesis. *EMBO J.* **23**: 950–958.
49. Robichon, C., M. Varret, X. Le Liepvre, F. Lasnier, E. Hajdouch, P. Ferre, and I. Dugail. 2006. DnaJA4 is a SREBP-regulated chaperone involved in the cholesterol biosynthesis pathway. *Biochim. Biophys. Acta.* **1761**: 1107–1113.
50. Mathur, S. N., K. R. Watt, and F. J. Field. 2007. Regulation of intestinal NPC1L1 expression by dietary fish oil and docosahexaenoic acid. *J. Lipid Res.* **48**: 395–404.
51. Fabricant, M., and S. A. Broitman. 1990. Evidence for deficiency of low density lipoprotein receptor on human colonic carcinoma cell lines. *Cancer Res.* **50**: 632–636.
52. Mann, M. J., and L. M. Hendershot. 2006. UPR activation alters chemosensitivity of tumor cells. *Cancer Biol. Ther.* **5**: 736–740.